Effect of solution temperature and absorber pressure in R134a–DMAC system using horizontal tubular absorbers

L. Harikrishnan, Shaligram Tiwari and M.P. Maiya*

Refrigeration and Air-conditioning Laboratory, Department of Mechanical Engineering, Indian Institute of Technology Madras, Chennai 600 036, India

Abstract

Investigations are carried out to study the heat and mass transfer characteristics of a falling film horizontal absorber by employing a two-dimensional numerical technique. The potential refrigerant, R134a (1,1,1,2-tetrafluroethane), is absorbed by the falling film of the R134a–DMAC (dimethylacetamide) solution. The variations of performance parameters along the tube surface are presented for different solution inlet temperatures and absorber pressures. The mass flux at the interface is observed to be higher at higher solution temperature and absorber pressure. The variation of the interface to bulk fluid and bulk fluid to wall heat transfer coefficient, overall heat transfer coefficient and mass transfer coefficient are studied for different solution temperatures and absorber pressures.

Keywords: falling film horizontal tubular absorber; R134a–DMAC; absorption characteristics; absorber pressure; solution temperature

*Corresponding author:
mpmaiya@iitm.ac.in

Received 1 June 2011; revised 18 October 2011; accepted 7 November 2011

1 INTRODUCTION

The vapor absorption refrigeration systems have strong potential to offer low carbon applications to the future refrigeration and air-conditioning industries. They are expected to cater to most of the needs in economical- and environment-friendly manner if appropriate refrigerant–absorbent pairs are identified. However, the attempt to investigate the new potential refrigerant–absorbent fluid pair would bank on the optimization of the basic principle of operation of the vapor absorption refrigeration systems and also of the components involved. The present work identifies the absorber of such a system as one of the critical components which offers the scope for performance improvement. There have been numerous experimental and numerical studies in literature devoted to analysis of the absorption phenomenon, but the scope for improving performance of the absorber still remains open. Deriving motivation from numerical approaches of analysis adopted in literature, the present study focuses on a particular refrigerant–absorbent fluid pair (R134a–DMAC) to study the characteristic behavior of absorption in a falling film absorber. The fluid pair is chosen only due to the ease of accessing their property values from literature. However, the method and qualitative inferences can be extended to any potential fluid pairs.

Killion and Garimella [1] explained the modeling technique developed by researchers for both non-volatile and volatile absorbents. They pointed out that although ammonia–water systems have been studied more than water–lithium bromide systems, the state-of-the-art numerical modeling techniques are not as much developed as those for water–lithium bromide systems. Grossman [2] studied numerically the combined heat and mass transfer process associated with the absorption of a vapor into a laminar liquid film. The energy and diffusion equations were solved simultaneously to give the temperature and concentration variations at the liquid–vapor interface and at the tube wall surface. His numerical solutions correspond to a linear temperature–concentration equilibrium relation with the assumption of constant heat of absorption. The results were presented for two cases of practical importance, viz. constant temperature and adiabatic wall conditions. Yang and Wood [3] developed a numerical model for simultaneous heat and mass transfer in smooth falling film absorption. They did not assume the linear absorbent assumption for the equilibrium as considered by Grossman [2]. Instead, the empirical thermodynamic equilibrium relations were employed, which make the non-dimensionalization less difficult. The results predicted were found to be in good agreement with those from more complicated formulations and the experimental data in the literature.

International Journal of Low-Carbon Technologies 2013, 8, 20–28
© The Author 2011. Published by Oxford University Press. All rights reserved. For Permissions, please email: journals.permissions@oup.com
doi:10.1093/ijlct/ctr042 Advance Access Publication 21 December 2011

Downloaded from https://academic.oup.com/ijlct/article-abstract/8/1/20/740792 by guest on 10 June 2020

A physical model was presented by Choudhury *et al.* [4] to analyze the absorption phenomenon in an actual situation for absorption of water vapor in water–LiBr solution. They reported that for higher solution flow rates, the heat transfer coefficient improves with an increase in the tube diameter and for smaller solution flow rates for given tube diameter, the heat transfer coefficient is relatively larger. A numerical study was carried out by Babadi and Farhanieh [5] to investigate the characteristics of falling film water–LiBr solution on a completely wetted horizontal tube. Boundary layer assumptions were used for the transport of mass, momentum and energy equations and the finite difference method was employed to solve the governing equations. The effect of basic flow parameters was investigated on the heat and mass transfer mechanism through the average Sherwood and Nusselt numbers. Based on the numerical data, two correlations were suggested for estimating the average heat and mass transfer coefficients of the transport phenomena over the tube.

Numerical studies had been carried out by Arivazhagan *et al.* [6] on R134a–DMAC-based half-effect absorption in solar energy-operated cold storage systems. When compared with ammonia–water, the R134a–DMAC pair was better for a half-effect system from the viewpoint of coefficient of performance (COP), second law of efficiency and source temperature for solar energy-based cold storage systems. From these results, it is evident that the R134a–DMAC refrigerant–absorbent combination may be considered as one of the favorable working fluid pairs when the half-effect system is to be operated with low-temperature heat sources. An experimental investigation was also conducted by Arivazhagan *et al.* [7] on the performance of a two-stage half-effect vapor absorption cooling system. The prototype was designed for 1-kW cooling capacity using R134a as a refrigerant and DMAC as an absorbent. The optimum generation temperature was in the range of 65–70°C. For the generator temperature of 70°C, a COP value of 0.36 was obtained.

Experimental studies on R134a–DMAC hot water-based vapor absorption refrigeration system were carried out by Muthu *et al.* [8]. They reported that with an increase in the heat source temperature, the quantities such as solution heat exchanger effectiveness, absorber effectiveness and generator effectiveness increase with an increase in the heat source temperature. More recently, experimental studies on heat and mass transfer performance of a coiled tube absorber were carried out by Mohideen and Renganarayanan [9] for an R134a–DMAC-based absorption cooling system. The optimum overall heat transfer coefficient of the system was found to be 726 $W\,m^{-2}\,K^{-1}$ for a film Reynolds number of 350.

The absorber characteristics had a significant effect on the overall efficiency of absorption machines studied by Deng and Ma [10] on the results of experimental data for a falling film absorber which was made up of 24-row horizontal smooth tubes. The effect of cooling water inlet temperature on the absorber's performance was found to be significant. As the inlet temperature of the cooling water decreases from 32 to 30°C, the heat flux of the absorber increases by more than 17%. The inlet solution concentration of lithium bromide was one of the most important parameters that influence the heat transfer coefficient. Experimental study was conducted by Yoon *et al.* [11] on the heat and mass transfer characteristics of a water–LiBr horizontal tube absorber made of small-diameter tubes. Three different tube diameters of 15.88, 12.7 and 9.52 mm, respectively, were considered inside the absorber to investigate the effect of the tube diameter on the absorber performance. Among the three different tube diameters considered, the smallest tube diameter of 9.52 mm shows the highest value of heat and mass transfer coefficients. The heat and mass transfer coefficients increase with an increase in the solution flow rate, whereas the heat and mass fluxes increase as the solution flow rate and the cooling water velocity increase. Most recently, a numerical study was carried out by Harikrishnan *et al.* [12] to investigate the flow, heat and mass transfer behavior of a falling film horizontal absorber with R134a–DMAC as the working fluid pair. The variations of performance parameters along the tube surface for different solution flow rates and coolant temperatures are presented. They had reported the optimum solution flow rates for different tube sizes.

The objective of the present work is to numerically study the effect of solution temperature and absorber pressure on absorption in the R134a–DMAC system using horizontal tubular absorbers. The governing equations of momentum, energy and species transport are solved simultaneously using a finite difference method. The variation of the interface temperature, interface concentration, mass flux at the interface, heat flux at the wall surface, interface to bulk fluid heat transfer coefficient, bulk fluid to wall heat transfer coefficient, overall heat transfer coefficient and mass transfer coefficient along the tube surface for different solution temperatures and absorber pressures are studied in detail.

2 PROBLEM STATEMENT

A scheme of the geometrical configuration of a falling film horizontal tubular model is shown in Figure 1. The weak solution is introduced at the top of the tube surface. It flows

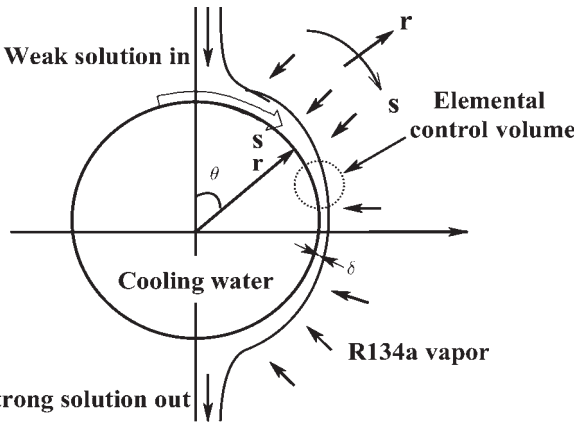

Figure 1. *Schematic representation of the solution film on the tube surface.*

Downloaded from https://academic.oup.com/ijlct/article-abstract/8/1/20/740792 by guest on 10 June 2020

around the curved surface of the tube resulting in change of film thickness. The R134a vapor is absorbed at the interface of the solution film and vapor and it diffuses into the solution film. Cooling water flowing inside the horizontal tube carries away the heat of absorption. Since the analysis is carried out at a particular cross-section of the tube, the tube surface is considered as an isothermal wall. In the parametric study, while changing solution temperature and absorber pressure, the solution flow rate is kept at 0.015 kg m^{-1} s^{-1} and the tube surface temperature at 25°C, respectively. The following assumptions have been made in the study of heat and mass transfer characteristics:

(1) The flow is laminar and no interfacial waves are present.
(2) The solution exhibits 100% wettability on the tube surface.
(3) The interface between the solution film and vapor is assumed to be in thermodynamic equilibrium.
(4) Physical properties are constant inside the domain. These have been evaluated at the inlet solution concentration and the mean film temperature. The mean film temperature is taken as the average of solution inlet temperature and coolant tube surface temperature.
(5) Heat transfer from the interface to the vapor phase is negligible.
(6) The variation of film thickness due to absorption of R134a vapor is small.
(7) The interface of solution and vapor is a shear-free surface.
(8) The outer surface temperature of the tube equals the bulk coolant temperature. Also, the conduction resistance of the tube is assumed to be negligible.

3 GOVERNING EQUATIONS AND BOUNDARY CONDITIONS

3.1 Governing equations

The energy and species transport equations are expressed as follows

$$u\frac{\partial T}{\partial s}+v\frac{\partial T}{\partial r}=\alpha\frac{\partial^2 T}{\partial r^2} \tag{1}$$

$$u\frac{\partial \omega}{\partial s}+v\frac{\partial \omega}{\partial r}=D\frac{\partial^2 \omega}{\partial r^2} \tag{2}$$

where u is the velocity in s-direction (m s^{-1}), T temperature (K), s the tangential coordinate along solution flow direction (m), v the velocity in r-direction (m s^{-1}), r the local radial coordinate normal to solution flow direction (m), α thermal diffusivity ($m^2 s^{-1}$), ω concentration and D the diffusion coefficient (m^2 s^{-1}).

Table 1. *Summary of boundary conditions.*

Boundary	Imposed boundary conditions
At the inlet	$T = T_{in}$ and $\omega = \omega_{in}$
On the tube wall surface	$T = T_w$ and $\frac{\partial \omega}{\partial r} = 0$
At the liquid–vapor interface	$\dot{m} = \frac{\rho D}{(1-\omega_{if})}\frac{d\omega}{dr}$ and $T_{if} = f(p, \omega_{if})$ also, $\dot{q} = \dot{m}_v h_{ab} = k\frac{dT}{dr}$

The tangential and normal velocity components of the falling film, 'u' and 'v', are expressed as [4, 14]

$$u=\frac{g}{2\upsilon}\sin\theta[2\delta(r-r_i)-(r-r_i)^2] \tag{3}$$

$$v=-\frac{g}{2\upsilon}(r-r_i)^2\left[\frac{d\delta}{ds}\sin\theta+\frac{1}{r_i}\cos\theta\left(\delta-\frac{r-r_i}{3}\right)\right] \tag{4}$$

where g is the acceleration due to gravity (m s^{-2}), υ kinematic viscosity (m^2 s^{-1}), θ the angle and δ film thickness (m). The variation of $(r_o - r_i)$ or δ, the film thickness, for the known solution flow rate, is expressed as

$$r_o - r_i = \delta = \left[\frac{3\mu\Gamma}{\rho^2 g\sin\theta}\right]^{1/3} \tag{5}$$

where μ is the dynamic viscosity (N s m^{-2}), Γ the solution flow rate (kg m^{-1} s^{-1}) and ρ density (kg m^{-3}).

Also, the variation of film thickness in the film flow direction is expressed from Equation (5) as,

$$\frac{d\delta}{ds}=-\left(\frac{\mu\Gamma}{9\rho^2 g}\right)^{1/3}\frac{1}{r_i}\frac{1}{\{\sin(s/r_i)\}^{1/3}\tan(s/r_i)} \tag{6}$$

3.2 Boundary conditions

The boundary conditions employed in the numerical solution of Equations (1) and (2) are summarized in Table 1. The enthalpy of absorption, h_{ab}, is expressed as follows

$$h_{ab} = h_v - h_s + \omega_s\left[h_r - h_d + \left.\frac{dh_E}{d\omega_s}\right|_{T_s}\right] \tag{7}$$

where h_r is enthalpy of R134a (kJ/kg), h_d is enthalpy of DMAC (kJ/kg) and h_E is excess enthalpy of solution (kJ/kg).

3.3 Expressions for heat and mass transfer coefficients

The variation of local heat transfer coefficient from the interface to bulk solution in the direction of film flow in terms of

Downloaded from https://academic.oup.com/ijlct/article-abstract/8/1/20/740792 by guest on 10 June 2020

Nusselt number is expressed as

$$Nu_{ib} = \frac{h_{ib}\delta}{k_s} = \frac{\delta}{(T_{if} - T_{bs})}\frac{dT}{dr}\bigg|_{r=r_o} \quad (8)$$

where k is the thermal conductivity ($W\,m^{-1}\,K^{-1}$), T_{bs} is Bulk solution temperature (K).

The variation of local heat transfer coefficient from the bulk solution to tube wall surface along the film flow in terms of Nusselt number is expressed as

$$Nu_{bw} = \frac{h_{bw}\delta}{k_s} = \frac{\delta}{(T_{bs} - T_w)}\frac{dT}{dr}\bigg|_{r=r_i} \quad (9)$$

The variation of local overall heat transfer coefficient with neglected film resistance is expressed with the help of Equations (8) and (9) as

$$U_i = \frac{1}{(1/h_{bw}) + (1/h_{ib})} \quad (10)$$

The variation of local mass transfer coefficient from the interface to bulk solution along the film flow is expressed in terms of Sherwood number as

$$Sh = \frac{h_m\delta}{D} = \frac{\dot{m}'\delta}{D\rho(\omega_{if} - \omega_{bs})} \quad (11)$$

where $\dot{m}'$ is the calculated mass flux ($kg\,m^{-2}\,s^{-1}$).

4 NUMERICAL SOLUTION TECHNIQUE

The geometrical configuration of the falling film on the horizontal tube is shown in Figure 1. The film thickness varies along the tube half-circumference in the downstream direction of the flowing solution film. To make the computational domain rectangular, coordinate transformation proposed by Choudhury *et al.* [4] has been adopted. For transformation of coordinates, non-dimensional variables, ξ and ζ, are considered in the film flow direction and in the perpendicular direction of film flow, respectively. Consequently, the respective governing equations and boundary conditions have been transformed using the non-dimensional transformation variables. A cosine grid has been employed to make the grid finer near the tube surface and near the interface where steep variations of gradients are expected. The discretization of governing equations and detailed numerical technique employed to find the temperature and concentration distributions in the flow field have been explained by Harikrishnan *et al.* [12].

5 RESULTS AND DISCUSSION

The range of parameters used to study the effect of performance characteristics of absorption process has been shown in Table 2

Table 2. *Range of input parameters.*

Parameters	Symbol	Range	Mean value
Coolant temperature (°C)	t_c	—	25
Mass flow rate of solution ($kg\,m^{-1}\,s^{-1}$)	Γ	—	0.015
Pressure (bar)	p	1–5	3
Solution inlet temperature (°C)	t_{in}	40–60	50
Tube size (mm)	d_t	—	12.7

Table 3. *Range of property values.*

Property name	Symbol	Range
Density ($kg\,m^{-3}$)	ρ	953.95–1063.52
Diffusion coefficient ($m^2\,s^{-1}$)	D	1.029×10^{-9}–1.104×10^{-9}
Dynamic viscosity ($N\,s\,m^{-2}$)	μ	7.06×10^{-4}–8.44×10^{-4}
Enthalpy of absorption ($kJ\,kg^{-1}$)	h_{ab}	160.88–184.99
Enthalpy of solution ($kJ\,kg^{-1}$)	h_s	453.46–483.04
Enthalpy of vapor ($kJ\,kg^{-1}$)	h_v	650.17–658.92
Kinematic viscosity ($m^2\,s^{-1}$)	υ	6.64×10^{-7}–8.85×10^{-7}
Specific heat ($J\,kg^{-1}\,K^{-1}$)	C_p	1809.58–2150.63
Thermal conductivity ($W\,m^{-1}\,K^{-1}$)	k	0.1232–0.1462
Thermal diffusivity ($m^2\,s^{-1}$)	α	6.402×10^{-8}–7.13×10^{-8}

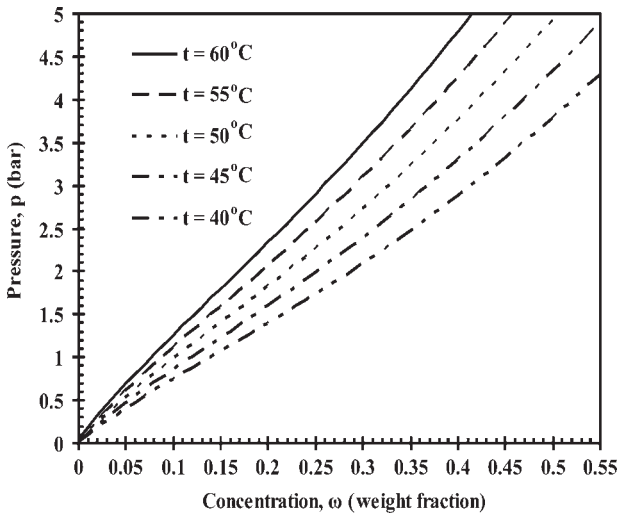

Figure 2. *Variation of pressure with solution concentration for different solution temperatures.*

and the range of property values considered is shown in Table 3. All the properties are calculated with the help of expressions given in the literature [15–19]. Since the parameters considered for the present study are solution temperature and absorber pressure, the equilibrium concentration also varies at the inlet. The respective equilibrium concentration is obtained from the PTX chart presented in Figure 2 for the known values of the solution inlet temperature and the absorber pressure. The computational code developed by Harikrishnan *et al.* [12] has been used to investigate the effect of absorber pressure and solution

Downloaded from https://academic.oup.com/ijlct/article-abstract/8/1/20/740792 by guest on 10 June 2020

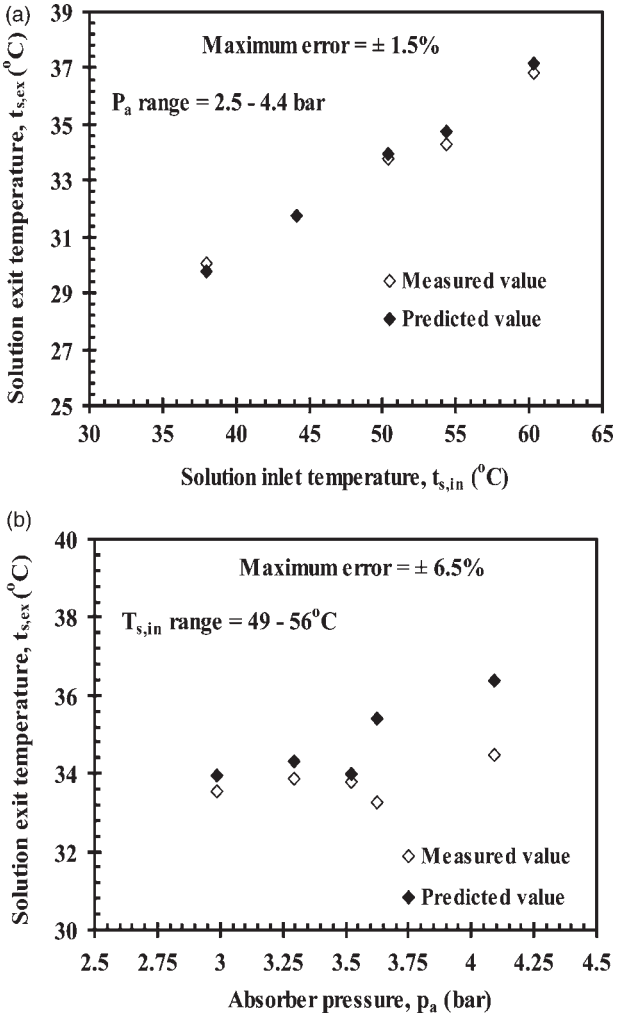

Figure 3. *Validation of model against the experimental data with (**a**) solution inlet temperature and (**b**) absorber pressure.*

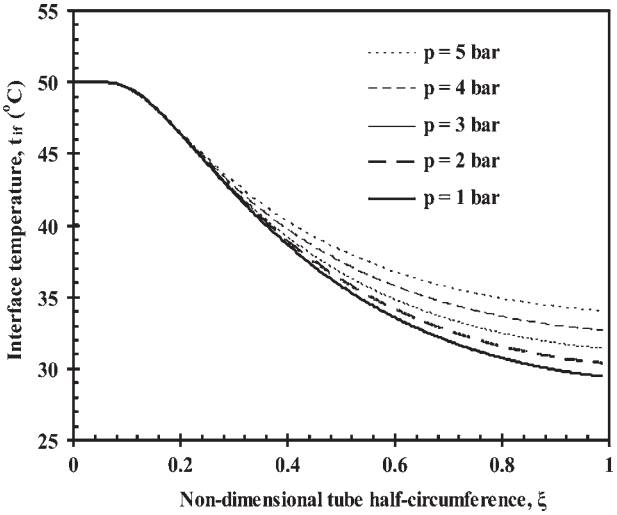

Figure 4. *Variation of the interface temperature along the tube surface for different absorber pressures.*

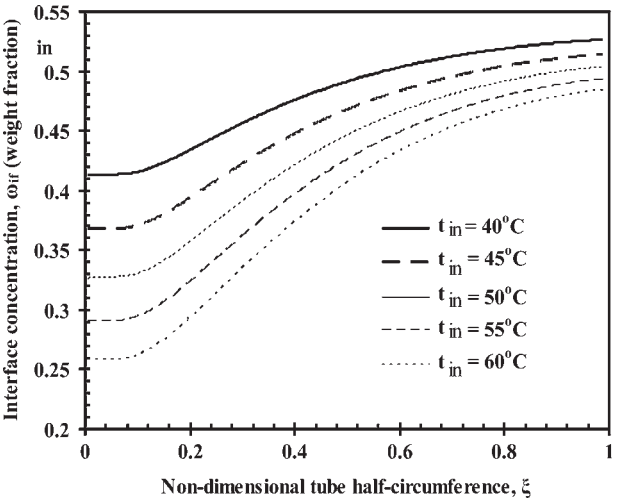

Figure 5. *Variation of the interface concentration along the tube surface for different solution temperatures.*

temperature. Figure 3a and b presents the validation of the model against the experimental data presented by Harikrishnan *et al.* [13]. The predicted solution exit temperature from the model is validated against the measured solution exit temperature from the tube in the first row of the falling film horizontal tubular absorber. It can be seen that the maximum error between the predicted solution exit temperature and the measured exit temperature is around 6.5%.

Figure 4 presents the variation of interface temperature along the tube surface for different values of absorber pressure. For a fixed solution temperature, at higher absorber pressure, the equilibrium solution inlet concentration would be higher. Moreover, at higher absorber pressure, the diffusion rate of R134a vapor into the solution film is higher. Consequently, an increased absorption rate results in higher heat of absorption liberated at the interface which increases the interface temperature at a particular angular position on the tube surface. Thus, at higher absorber pressure, the interface gets relatively more heated when compared with lower absorber pressure at a given angular position on the tube surface and for fixed value of the inlet temperature. It is observed from Figure 4 that the interface temperature lying beyond the boundary layer almost remains constant till $\xi = 0.1$, i.e. up to 10% of the circumferential length.

Figure 5 presents the variation of interface concentration along the tube surface for different values of solution temperature. Higher solution temperature is associated with lower inlet concentration for given absorber pressure and causes the interface concentration to decrease. Lower solution inlet concentration leading to higher absorption rate of the vapor increases the gradient of interface concentration along the tube surface. On the other hand, a higher solution concentration is associated with lower solution temperature which causes a decrease in the absorption rate of R134a vapor along the tube surface.

Downloaded from https://academic.oup.com/ijlct/article-abstract/8/1/20/740792 by guest on 10 June 2020

This is apparent from the figure that shows decreasing concentration gradient along the tube surface. No variation of concentration at the interface is observed until $\xi = 0.1$ due to very small absorption. The variation of both interface temperature and interface concentration is quite small till $\xi = 0.1$ due to the assumed vapor–liquid equilibrium at the interface.

Figure 6a presents the variation of mass flux at the interface along the tube surface for different solution inlet temperatures. Higher solution temperature is associated with lower solution inlet concentration which gives rise to a higher absorption rate of R134a vapor and increased mass flux. The mass flux increases till a particular angular position of the tube surface, attains its peak value and then begins to decrease. The peak of mass flux variation gets shifted to further downstream locations with an increase in solution inlet temperature. Figure 6b presents the variation of heat flux at the tube wall surface along the tube surface for different solution inlet temperatures. The heat flux at the tube surface is very high at the inlet due to much smaller thickness of the thermal boundary layer. It is observed to be higher for higher solution inlet temperature and vice versa. The higher value of inlet solution temperature increases the temperature gradient between bulk solution and tube surface causing an increase in heat transfer and heat flux.

The variation of mass flux along tube surface for different absorber pressures is presented in Figure 7a. It shows that the mass flux is higher for higher value of absorber pressure. The diffusion rate of R134a vapor into the solution film increases at higher absorber pressure resulting in increased mass flux. For an absorber pressure of 1 bar, the nature of variation of mass flux is almost flat. With an increase in absorber pressure, the nature of variation changes and the peak location occurs between $\xi = 0.5$ and $\xi = 0.6$. This peak location gets shifted upstream with an increase in absorber pressure. Figure 7b shows the variation of heat flux along the tube surface for different values of absorber pressure. At higher absorber pressure,

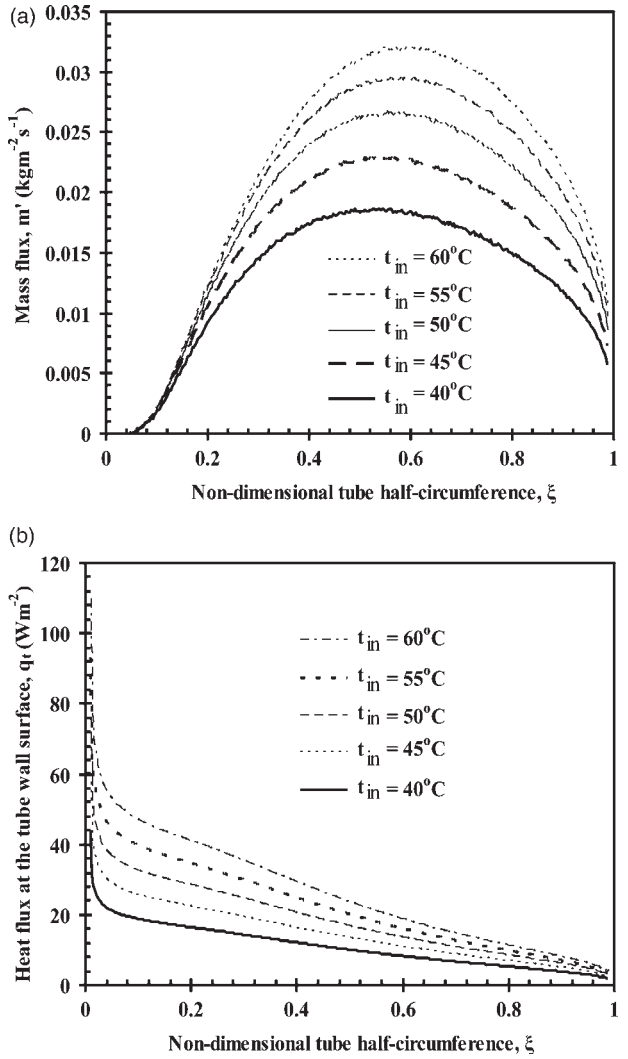

Figure 6. *Variation of (**a**) mass flux at the interface and (**b**) heat flux at the tube wall surface, along the tube surface for different solution inlet temperatures.*

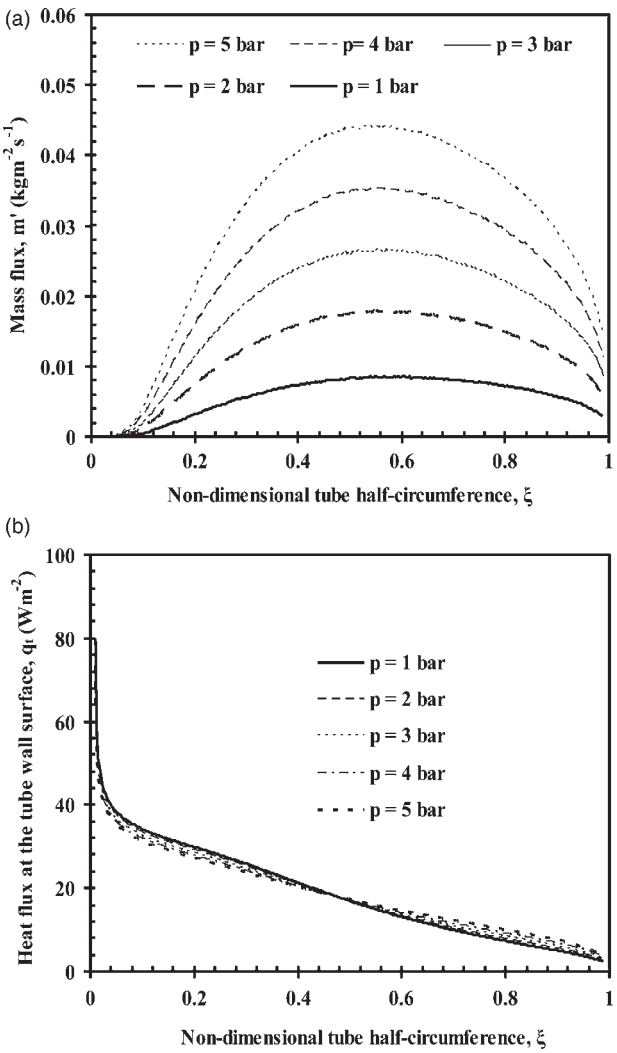

Figure 7. *Variation of (**a**) mass flux at the interface and (**b**) heat flux at the tube wall surface, along the tube surface for different absorber pressures.*

Downloaded from https://academic.oup.com/ijlct/article-abstract/8/1/20/740792 by guest on 10 June 2020

the heat flux at the tube surface is less than that for lower absorber pressure till $\xi = 0.5$, beyond which it is observed to show reversed nature of variation.

Figures 8 and 9 present the variation of transfer coefficients along tube surface for different values of solution temperature. The values of interface to bulk fluid and overall heat transfer coefficient are found to be lower for higher solution temperatures and vice versa. At a higher solution temperature, the interface to bulk fluid heat transfer coefficient decreases due to a decrease in temperature gradient at the interface. The peak value of interface to bulk fluid heat transfer coefficient is reached at $\xi = 0.7$ and is higher at the same location for higher solution temperature. A similar trend is observed for the local variation of the overall heat transfer coefficient as well. The local value of bulk fluid to wall heat transfer coefficient is higher at the inlet and reaches its minimum value within $\xi = 0.1$ and then increases gradually to attain a maximum value around $\xi = 0.5$ after which it further decreases. For higher solution temperature, the bulk fluid to wall heat transfer coefficient increases resulting in increased heat transfer rate. The local mass transfer coefficient is found to be higher for lower solution temperature and vice versa. In general, the local mass transfer coefficient decreases along the tube surface.

Figures 10 and 11 present the variation of transfer coefficients along the tube surface for different values of absorber pressure. Except bulk fluid to wall heat transfer coefficient, all other transfer coefficients are higher at higher absorber pressure. At higher absorber pressure, the interface to bulk fluid heat and mass transfer coefficients are observed to be higher due to increased heat and mass fluxes at the interface. With an increase in the absorber pressure, fluctuations occur in the computed mass transfer coefficient at further downstream locations. This is the reason why the starting position for variation

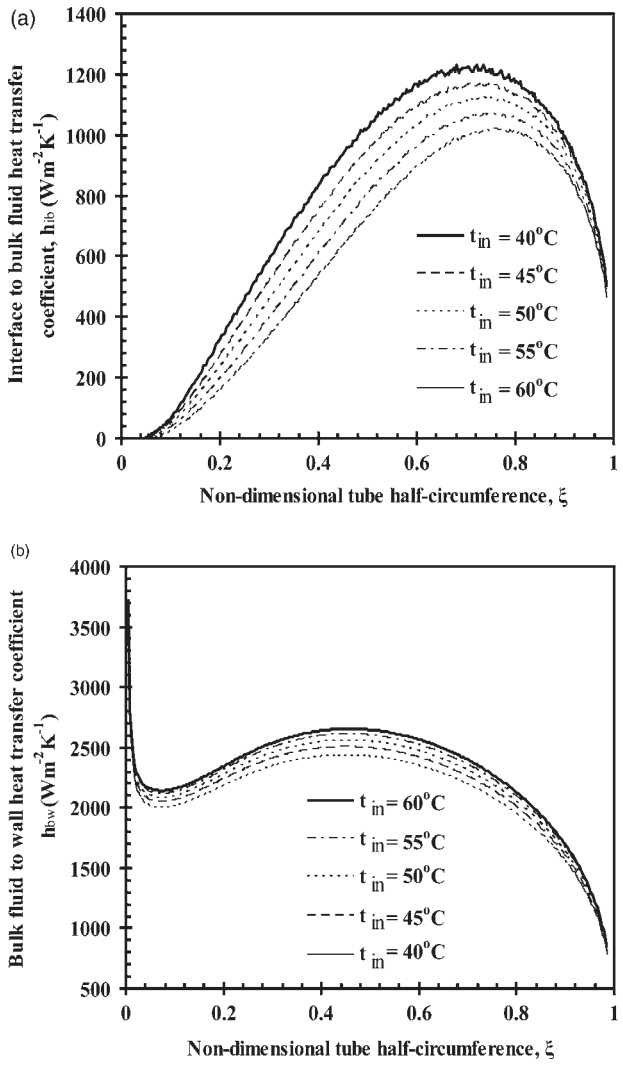

Figure 8. *Variation of (**a**) interface to bulk fluid and (**b**) bulk fluid to wall heat transfer coefficient, along the tube surface for different solution inlet temperatures.*

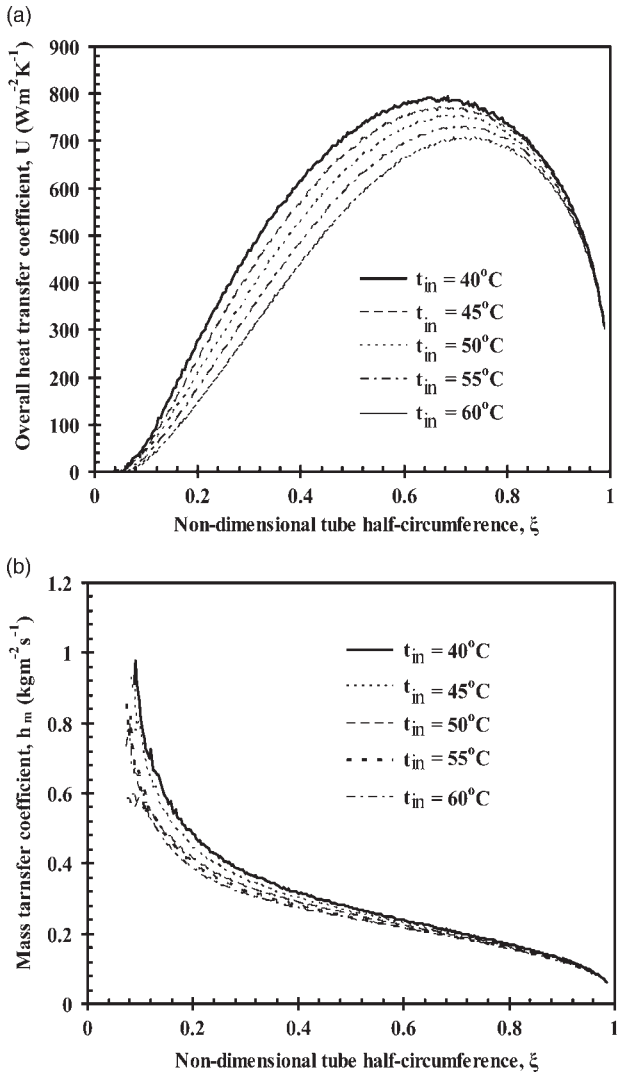

Figure 9. *Variation of (**a**) overall heat transfer coefficient and (**b**) mass transfer coefficient, along the tube surface for different solution inlet temperatures.*

Downloaded from https://academic.oup.com/ijlct/article-abstract/8/1/20/740792 by guest on 10 June 2020

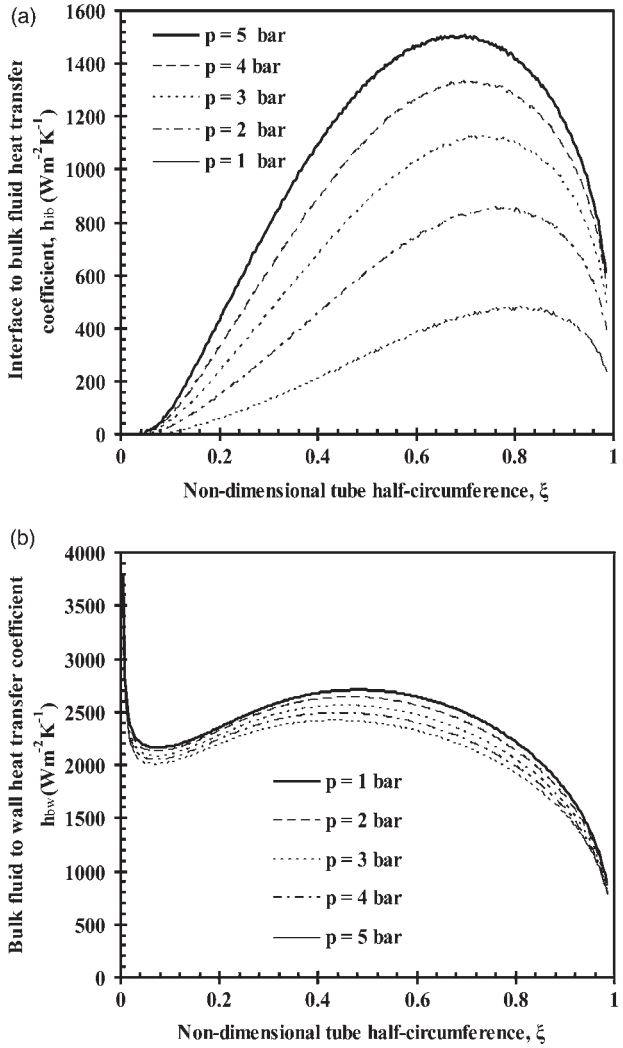

Figure 10. *Variation of (**a**) interface to bulk fluid and (**b**) bulk fluid to wall heat transfer coefficient, along the tube surface for different absorber pressures.*

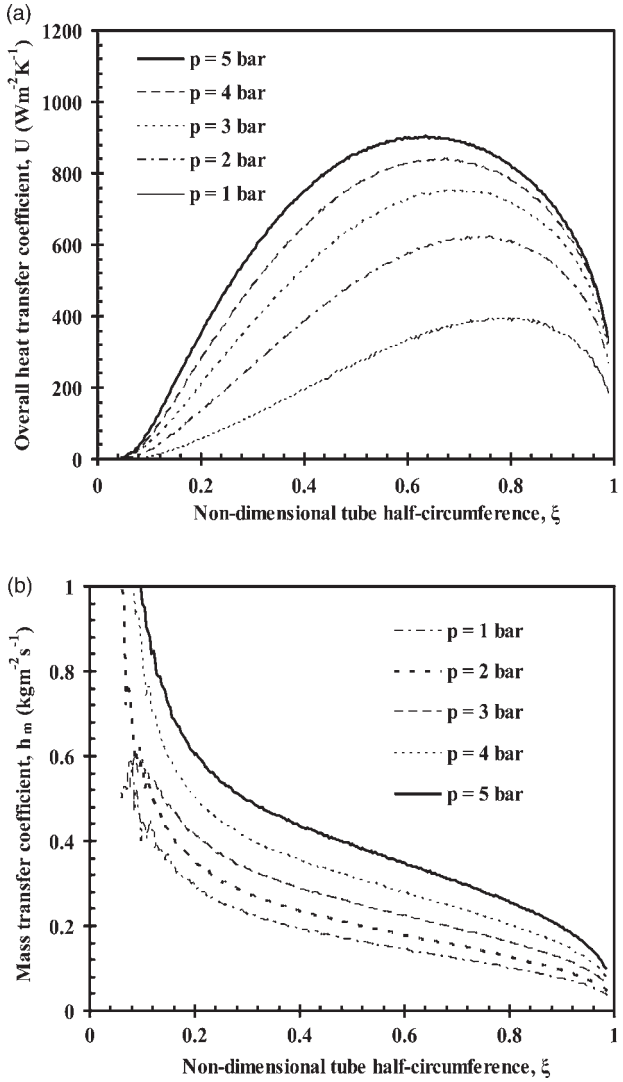

Figure 11. *Variation of (**a**) overall heat transfer coefficient and (**b**) mass transfer coefficient, along the tube surface for different absorber pressures.*

of mass transfer coefficient is chosen to be$\xi = 0.1$. The local overall heat transfer coefficient depends on interface to bulk fluid and bulk fluid to wall heat transfer coefficients. Consequently, the variation of overall heat transfer coefficient is similar to the nature of variation of interface to bulk fluid heat transfer coefficient. There is a significant variation in the peak value of interface to bulk fluid and overall heat transfer coefficients over the range of absorber pressure considered. The reason for decreasing bulk fluid to wall heat transfer coefficient with an increase in absorber pressure is attributed to the fact that the higher value of bulk solution temperature at a particular location on the tube surface gives rise to higher temperature difference between bulk fluid and tube surface.

It is apparent from the present study how the absorber pressure and solution inlet temperature affect the absorption rate of R134a vapor at the interface. The maximum amount of absorption rate required can be achieved by the state of solution (inlet temperature and concentration) when the absorber is maintained at a particular pressure. The area under the curves in Figure 6a give the total mass of R134a absorbed for a particular solution flow rate. Hence, the conditions at the inlet of the absorber can be found with the help of the present model to achieve a maximum absorption of R134a. Moreover, the outcomes of current work are useful in finding the effect of transfer coefficients that play an important role in deciding heat and mass transfer characteristics in the falling film absorption process.

6 CONCLUSIONS

This two-dimensional numerical study has been carried out using the cosine grid to investigate the heat and mass transfer characteristics of R134a–DMAC in a falling film horizontal tube absorber. The results show that higher value of solution

Downloaded from https://academic.oup.com/ijlct/article-abstract/8/1/20/740792 by guest on 10 June 2020

temperature is associated with lower solution inlet concentration that gives rise to higher absorption rate of R134a vapor and increased mass flux. Higher solution inlet temperature increases temperature gradient between bulk solution and tube surface which increases heat transfer coefficient as well as heat flux. However, for higher absorber pressure, the heat flux at the tube surface is small up to around 50% of tube half-circumference and then begins to increase. The interface to bulk fluid heat transfer coefficient, overall heat transfer coefficient and mass transfer coefficient are found to be lower for higher solution temperature and vice versa. At higher solution temperature, the bulk fluid to wall heat transfer coefficient is higher. The important observation made from the present study confirms that with an increase in absorber pressure, the nature of variation of all the transfer coefficients is opposite when contrasted with the effects caused due to increased solution temperature.

REFERENCES

[1] Killion JD, Garimella S. A critical review of models of coupled heat and mass transfer in falling-film absorption. *Int J Refrig* 2001;**24**:755–97.

[2] Grossman G. Simultaneous heat and mass transfer in film absorption under laminar flow. *Int J Heat Mass Transfer* 1982;**26**:357–71.

[3] Yang R, Wood BD. A numerical modeling of an absorption process on a liquid falling film. *Solar Energy* 1992;**48**:195–8.

[4] Choudhury SK, Hisajima D, Ohuchi T, *et al.* Absorption of vapors into liquid film flowing over cooled horizontal tubes. *ASHRAE Trans* 1993;**99**:81–9.

[5] Babadi F, Farhanieh B. Characteristics of heat and mass transfer in vapor absorption of falling film flow on a horizontal tube. *Int Commun Heat Mass Transfer* 2005;**32**:1253–65.

[6] Arivazhagan S, Murugesan SN, Saravanan R, *et al*. Simulation studies on R134a–DMAC based half effect absorption cold storage systems. *Energy Convers Manage* 2005;**46**:1703–13.

[7] Arivazhagan S, Saravanan R, Renganarayanan S. Experimental studies on HFC based two stage half effect vapour absorption cooling system. *Appl Thermal Eng* 2006;**26**:1455–62.

[8] Muthu V, Saravanan R, Renganarayanan S. Experimental studies on R134a–DMAC hot water based vapour absorption refrigeration systems. *Int J Thermal Sci* 2008;**47**:175–81.

[9] Mohideen TS, Renganarayanan S. Experimental studies on heat and mass transfer performance of a coiled tube absorber for R134a/DMAC based absorption cooling system. *Heat Mass Transfer* 2008;**45**:47–54.

[10] Deng SM, Ma WB. Experimental studies on the characteristics of an absorber using LiBr–H_2O as working fluid. *Int J Refrig* 1999;**22**:293–301.

[11] Yoon JI, Phan TT, Moon CG, *et al*. Heat and mass transfer characteristics of a horizontal tube falling film absorber with small diameter tubes. *Heat Mass Transfer* 2008;**44**:437–44.

[12] Harikrishnan L, Tiwari S, Maiya MP. Numerical study of heat and mass transfer characteristics on a falling film horizontal tubular absorber for R134a–DMAC. *Int J Thermal Sci* 2011;**50**:149–59.

[13] Harikrishnan L, Maiya MP, Tiwari S. Investigations on heat and mass transfer characteristics of falling film horizontal tubular absorber. *Int J Heat Mass Transfer* 2001;**54**:2609–17.

[14] Bird RB, Stewart WE, Lightfoot EN. *Transport Phenomena*, 1st edn. John Wiley and Sons, 1960.

[15] Borde I, Stephan K. Search for alternative working fluid free of CFCs for the refrigeration, air conditioning and energy recovery industry. Final scientific report to the German Israeli Foundation for Scientific Research and Development, I-124-042.10/89.

[16] Reid RC, John MP, Bruce EP. *The Properties of Gases and Liquids*, 4th edn. McGraw-Hill, 1987.

[17] Arora CP. *Refrigeration and Air-Conditioning*, 2nd edn. Tata McGraw-Hill, 2004.

[18] Wilson DP, Basu RS. Thermodynamic properties of a new stratospherically safe working fluid—refrigerant 134a. *ASHRAE Trans* 1988;**94**:2095–118.

[19] Yokozeki A. Theoretical performance of various refrigerant–absorbent pairs in a vapor-absorption refrigeration cycle by the use of equations of state. *Appl Energy* 2005;**80**:383–99.

Downloaded from https://academic.oup.com/ijlct/article-abstract/8/1/20/740792 by guest on 10 June 2020